

PCCP

Accepted Manuscript



This is an *Accepted Manuscript*, which has been through the Royal Society of Chemistry peer review process and has been accepted for publication.

Accepted Manuscripts are published online shortly after acceptance, before technical editing, formatting and proof reading. Using this free service, authors can make their results available to the community, in citable form, before we publish the edited article. We will replace this *Accepted Manuscript* with the edited and formatted *Advance Article* as soon as it is available.

You can find more information about *Accepted Manuscripts* in the [Information for Authors](#).

Please note that technical editing may introduce minor changes to the text and/or graphics, which may alter content. The journal's standard [Terms & Conditions](#) and the [Ethical guidelines](#) still apply. In no event shall the Royal Society of Chemistry be held responsible for any errors or omissions in this *Accepted Manuscript* or any consequences arising from the use of any information it contains.

**Combinatorial Effect of Rolling and Carbonaceous Nanoparticles on the
Evolution of Crystallographic Texture and Structural Properties of
Ultra High Molecular Weight Polyethylene**

K. Elayaraja, Rajib Kalsar, Suryasarathi Bose, Satyam Suwas and Kaushik Chatterjee*

Department of Materials Engineering

Indian Institute of Science, Bangalore 560012 India

**author to whom correspondence should be addressed:*

E-mail: kchatterjee@materials.iisc.ernet.in

Abstract

Ultra high molecular weight polyethylene (PE) is a structural polymer widely used in biomedical implants. The mechanical properties of PE can be improved either by controlled crystalline orientation (texture) or by the addition of reinforcing agents. However, the combinatorial effect has not received much attention. The objective of this study was to characterize the structure and mechanical properties of PE composites incorporating multiwall carbon nanotubes (MWCNT) and reduced graphene oxide (RGO) subject to hot rolling. The wide angle X-ray diffraction studies revealed that mechanical deformation resulted in a mixture of orthorhombic and monoclinic crystals. Further, the presence of nanoparticles resulted in lower crystallinity in PE with smaller crystallite size, more so in RGO than in MWCNT composites. Rolling strengthened the texture of both orthorhombic and the monoclinic phases in PE. Presence of RGO weakened the texture of both phases of PE after rolling whereas MWCNT only mildly weakened the texture. This resulted in a reduction in elastic modulus of RGO composites whereas moduli of neat polymer and the MWCNT composite increased after rolling. This study provides new insight into the role of nanoparticles on texture evolution during polymer processing with implications for processing of structural polymer composites.

Keywords: Polymer nanocomposite; Texture; Ultra high molecular weight polyethylene; Graphene; Carbon nanotubes.

1. Introduction

The role of crystallographic texture on material properties is well documented for many engineering applications. Steels used in transformer cores, Zirconium tubes in nuclear reactors, Titanium alloys in aerospace applications and the epitaxial growth of superconductor thin films on Silicon wafers are some of the many applications where texture is routinely modulated to maximize material performance¹⁻³. Although, the effect of controlled crystalline orientation on structure-property relation in polymers is less understood, it offers a potential route to enhance their mechanical properties. There is a need to develop better understanding of texture evolution during processing of polymers and their composites for enhancing the mechanical properties for structural applications. Towards this goal, ultra high molecular weight polyethylene (PE) and its nanocomposites were taken as a model system in this study.

PE is widely used as acetabular cup lining and tibial insert in artificial hip joints owing to its bio-inertness and good mechanical properties⁴. However, these implants have a limited life due to the wear of PE components^{4, 5}. Accumulation of the wear debris causes inflammation, osteolysis and eventual loosening of the implant. It is estimated that over 150,000 total hip replacements are performed annually in the US alone⁶. A significant fraction of these surgeries are procedures performed to replace an implanted device that typically last about 15 years⁷. Thus, there is an unmet need to improve the mechanical properties of PE for the next generation of prosthetic joints with longer lives especially for more active, younger patients⁷.

Given its high molecular weight, limited solubility in solvents and the high viscosity of the melt, PE is a difficult material to process limiting the available options

for processing. A number of different approaches have been attempted to improve the mechanical properties of PE such as cross-linking⁸, blending⁹, irradiation¹⁰, and addition of micro/nano particles⁹, drawing/rolling¹¹, etc. The main disadvantages of cross-linking PE are the reduction of its fracture toughness and the generation of free radicals which leads to oxidation of the polymer¹². Irradiation can cause chain scission¹³. Since PE is one of the strongest polymers, blending does not yield significant improvements in mechanical properties. In more recent years, nanoparticles are being incorporated to enhance the mechanical strength and wear resistance of PE. Carbonaceous nanoparticles such as carbon nanotubes (CNT) and graphene exhibit exceptional mechanical properties, superior thermal and electric properties. As a result, they are being widely studied for reinforcing polymer matrices^{5, 14, 15}. Another strategy to improve the mechanical properties of structural polymers is through processing techniques such as drawing and rolling wherein strengthening is driven by controlled crystalline orientation (texture) in the rolling direction. Rolling/ drawing do not suffer from many of the limitations listed above and are widely used techniques for processing polymers industrially. Bahadur et al reported that mechanical properties of acetal, nylon 66, poly(vinyl chloride) and polycarbonate increased following cold rolling¹⁶. Rolling of polypropylene was also shown to significantly increase the Young's modulus.

In the recent past, controlled crystalline orientation and deformation of lamellar structure of rolled low density polyethylene (LDPE) and high density polyethylene (HDPE) were investigated by X-ray diffraction and scattering technique¹⁷⁻¹⁹. Anomalous mechanical and structural behaviors were observed on cold and hot drawn LDPE²⁰. For instance, structural changes along with change in the crystallite orientation and the

deformation of the lamellar structure in HDPE were investigated systematically by Yoda and Kuriyama²¹. Further, it has been reported that hot drawing yields higher Young's modulus than cold drawing of PE¹¹. Moreover, tensile strength of hot and quench rolled PE increased with increasing draw ratio²². Apart from controlled crystalline orientation, combination of roll-drawing and cross-linking of PE also showed significant wear resistance in a multidirectional wear analysis on smooth surface²³. It is envisaged that the texture of PE, often generated by rolling or drawing, results in microfibrillar morphology oriented along the rolling or drawing direction. In addition, the evolved microstructure show a decreased strength and increased toughness parallel to the tensile axis and increased strength and decreased toughness perpendicular to the tensile axis²⁴.

It is now well understood that the structural properties of PE can be enhanced by either addition of nanoparticles or through control of crystalline orientation. Industrially, rolling/drawing are among the most widely used processing techniques used for fabrication of and strengthening of PE-based products. In recent years, the use of nanoparticle-reinforced PE composites has been proposed. However, the effects, if any, of rolling of such PE nanocomposites has not been systematically studied. Therefore, the objective of this work was to investigate the combinatorial effect of addition of the nanoparticles followed by rolling of PE on the crystallographic changes and the resultant changes in structural properties. However, the combinatorial effects on the structure-property correlation have not received much attention. In view of this, it is pertinent to understand the combined effects of nanoparticles and crystallographic texture on the structural properties of PE based composites. The texture evolution in the polymer matrix in presence of the nanofillers was characterized to elucidate mechanisms underlying the

observed trends in mechanical properties assessed using dynamic thermal analysis and tensile tests. Furthermore, the phase transformation during rolling was systematically studied using X-ray diffraction and correlation of the observed phase transformation with the structural properties in the composites has been attempted.

2. Materials and Methods

2.1. Materials

PE ($M_w = 3 \times 10^6$ to 6×10^6) was purchased from Sigma Aldrich. Graphite flakes were obtained from Superior Company. Potassium permanganate Merck (KMnO_4 , 99.9%), sulfuric acid Merck (H_2SO_4 , 98%), phosphoric acid Merck (H_3PO_4 , 85%), hydrogen peroxide Merck (H_2O_2 , 30%), Hydrogen chloride (HCl , 37%) S-D Fine Chemicals and pristine multiwall carbon nanotubes (MWCNTs, NC7000, with average diameter of 9.5 nm and an average length of 1.5 μm) were purchased from Nanocyl. GO was prepared from graphite flakes by modified Hummer's method as reported previously²⁵. RGO was prepared by thermal reduction of GO as reported²⁵.

2.2. Processing and SEM characterization of composites

1 wt% RGO and 1 wt% MWCNTs were manually mixed with PE powder using pestle and mortar. Rectangular strips (50 mm length x 10 mm width x 1 mm thickness) of the neat polymer and the composites were prepared by a laboratory scale compression molding machine at 180° C. Hereafter, neat polymer, 1 wt% RGO composite and the 1 wt% MWCNT composites prepared by compression molding will be referred to as PE, GPE and CPE, respectively. Surface morphology of PE and the two composites was assessed using a scanning electron microscope (SEM) after cryo-fracturing in liquid nitrogen. The samples were sputter-coated with gold and imaged (FEI Sirion XL30 FEG).

In rolling, deformation takes place by plane strain condition. In the present case, the samples were pre-heated in a vacuum oven at 100° C for 4 h. Subsequently, strips were rolled at 100° C with a draw ratio of 1.5. Hereafter, rolled samples are referred to as PE-R, GPE-R and CPE-R. The samples were cyro-fractured to expose the cross-sectional

surface so as to visualize the morphology of the fibrils along the rolling direction and imaged as above.

2.3. XRD and texture measurements

The X-ray diffraction (XRD) patterns of unrolled and rolled neat and PE composites were recorded using PANalytical diffractometer with maximum power of 40kV/40mA, CuK_α (1.5406 Å) source, scanning speed of 1°/min and 2θ range between 10° to 60°. Bulk texture in the unrolled and rolled neat and PE composites were determined by XRD on the normal plane by Schulz reflection method. A Bruker D8 Discover X-ray texture goniometer with Ni-filtered CuK_α radiation was used for this. The (110), (200), and (020) reflections from the orthorhombic phase were analyzed to determine the texture of the unrolled samples. For the rolled samples (110), (200) and (020) reflections are for orthorhombic phase, and (001) reflection for monoclinic phase were recorded. All the pole figures were analyzed by MTEX (Matlab Texture analysis tool) software.

2.4. DMA analysis

The dynamic mechanical behavior of the unrolled and rolled samples was studied by DMA in the tension mode (MetraviB DMA 100). Rectangular specimens (20 mm x 6 mm x 1 mm) were used. The rolled samples were tested along the rolling direction. Storage modulus was obtained from the DMA analysis. All tests were performed at an oscillation frequency of 50 Hz at 25° C, pre-load of 2 N and dynamic force of 20 N.

3. Results and discussion

3.1. Phase transformation during rolling

PE is a semi-crystalline polymer that has been reported to undergo an allotropic transformation during mechanical deformation from orthorhombic ($D_{2h}^{16} - pmma$) to monoclinic ($C_{2h}^3 - C2/m$) crystal structure^{26, 27}. The lattice parameters reported for the two phases are compiled in Table 1²⁸. Figures 1(a) and 1(b) present the XRD patterns of unrolled and rolled polymer nanocomposites, respectively. Figures 1(c) and 1(d) compile the intensities of the major peaks. The (110), (200) and (020) peaks in Figure 1(a) are characteristic of the orthorhombic phase of PE. The addition of MWCNT and RGO did not result in any change in the crystal structure of PE. The XRD pattern of the rolled polymer, as displayed in Figure 1(b) indicates the formation of the monoclinic phase. It is envisaged that when the polymer is subjected to stress (tensile or compressive) beyond its yield point, the formation of monoclinic phase is facilitated. Any phase transformation arising from annealing prior to rolling, in the absence of mechanical deformation, was also studied in a control experiment where in samples were characterized after annealing without rolling. These experiments revealed that rolling but not annealing at the same temperature induces formation of the monoclinic phase. The mechanically driven phase transformation has been reported earlier²⁸. It is envisaged that in hot rolled samples, the crystallite orientation is random in the orthorhombic plane, the resulting monoclinic crystallites as well as the remaining orthorhombic crystallites are oriented with respect to the deformation axis. This phenomenon often leads to dislocations, disrupted crystals, and some chain unfolding. In metallic materials such transformation is observed in Austenite steels, NiTi alloys where the transformed phase is

the martensite phase. In martensitic transformation process, product and the parent phase bear a certain crystallographic orientation relationship. Such relationship is guided by the fact that the close packed plane and direction of the parent phase are parallel to the closed packed plane and direction of the product phase. In the present case, for orthorhombic to monoclinic phase transformation in PE, the orientation relationship is given by $(110)_o // (100)_m$ ²⁷. In Figure 2, the orientation relationship arising from orthorhombic to monoclinic transformations is shown schematically as stereographic projection. Thus, mechanical deformation but not nanoparticles induced phase transformation in PE.

Although there was no change in the crystal structure on addition of either MWCNT or RGO, there was a reduction in the intensity of the XRD peaks. The reduced intensity of the (110) and (200) peaks, as shown in Figures 1(c) and 1(d), indicate a decrease in the crystallinity of the polymer upon addition of nanoparticles in both unrolled and rolled samples. Inclusion of MWCNT led to decrease in the crystallinity of PE which was further reduced when RGO was used as a reinforcing agent. The intensity of the (001) peak of the new monoclinic phase developed during rolling was lower than the neat polymer itself in the rolled samples (Figure 1(d)).

The percentage crystallinity and average crystallite sizes were calculated for unrolled and rolled PE and the various nanocomposites studied here (Table 2). The percentage of the crystalline regions was calculated from XRD data as follows²⁹:

$$\% \text{ Crystallinity} = ((\text{Total area of XRD peak} - \text{Amorphous peak area}) / \text{Total area}) \times 100.$$

Crystallite size of unrolled and rolled PE was calculated using the Scherrer formula: $D = K \times \lambda / \beta \times \cos\theta$, where D is the crystallite size, λ is wavelength of incident X-rays, θ is the Bragg angle, β is the full width at half maximum of the diffraction peak

(radian) and K is constant ($K \approx 1$)²⁹. This calculation was done after the corrections for instrumental broadening and K_{α} doublet correction. These data indicate that the addition of the nanoparticles reduces the crystallite size as well as the crystallinity of the polymer. Therefore, the presence of nanoparticles leads to the formation of smaller and less perfect crystals. It is well known that MWCNT and RGO act as heteronucleating sites for crystallization and enhances the kinetics of crystallization³⁰. This often results in a broad distribution of spherulite size and defective crystals^{30, 31}. It is envisaged that two-dimensional plate-like morphology of RGO in contrast to two-dimensional tube-like morphology of MWCNTs facilitates more polymer-particle interactions in GPE than in CPE. Thus, GPE composites exhibited lower crystallinity and smaller crystallite size than CPE composites, both before and after rolling.

It was observed that the crystallite size marginally decreased in presence of the nanoparticles in the rolled samples. Interestingly, this observation is consistent for both orthorhombic and monoclinic crystals. In the case of rolling, the chain orientation in the crystalline and the amorphous regions are expected to increase which in turn leads to the formation of inter-crystalline linkages such as amorphous tie molecules and crystalline bridges. Semi-crystalline orthorhombic PE has total of eight slip systems, out of which four are independent. To fulfill the criterion for polycrystalline deformation total five independent slip systems are required. The additional deformation mechanism in the present case is attributed to shear in the amorphous phase³². It appears from XRD that, in presence of particles, formation of the inter-crystalline linkages are impeded, which in turn can have adverse consequences on the mechanical properties and is further discussed

below. To gain further insight on the effect of particles on the crystallographic texture, the crystal orientation of the rolled samples were studied in more detail.

3.2. Texture evolution

In the present investigation, two types of texture changes are observed (i) deformation texture (ii) transformation texture. Deformation texture evolves during rolling. Transformation texture in the present case is attributed to transformation of orthorhombic PE into monoclinic. Figures 3 and 4 present the pole figures for the polymer and its composites before and after rolling, respectively. RD, TD and ND refer to the three principal axes namely rolling direction, transverse direction and normal direction, respectively. The texture intensities are color coded as indicated in the colored scale bar. In the compression molded samples, prior to rolling, significantly strong texture was seen in the (110) and the (200) pole figures. In PE and the two composites, the (110) pole was distributed in all directions with maxima nearly coinciding with ND. Hot pressed PE, CPE and GPE show fiber type texture before rolling. Figures 5(a) and 5(b) present a comparison of the texture intensity. Note that inclusion of MWCNT and RGO in PE reduced the pole intensity in the (110) pole figure. Moreover, the texture of the polymer and the two composites are similar.

After deformation, $\{100\} \langle 001 \rangle$ type strong texture component was observed. Rolling led to significant changes in the crystallographic texture of the polymer matrix. The maxima of (110) pole in PE-R was distributed along both the TD and RD axis. Along the TD, the maxima ($\{100\} \langle 001 \rangle$ component) lay 55° away from ND whereas it lay 25° away from ND along the RD. However, a comparison of the intensities revealed that the maxima were sharper along the RD axis than along the TD axis. The presence of

the nanoparticles did not change the type of texture in the polymer. The (110) pole in both the composites were also distributed alongside the TD and the RD axis. The texture intensity in the CPE composite was similar to that of PE but was much lower in the RGO composites (Figure 5(a)).

The distribution of the maxima of the (200) pole also changed after rolling. In the rolled polymer the maxima lay 35° away from ND along the RD axis. The (001) pole of the monoclinic phase is also plotted in Figure 4. The monoclinic phase (001) pole was fiber type texture or (001) plane perpendicular to the ND axis. The addition of MWCNT and RGO did not change the distribution of texture. However, the texture intensity was lowered in the presence of RGO but not MWCNT relative to that of the rolled polymer (Figure 5(b)). Formation of deformation twinning in (310) and (110) plane could be responsible for texture transition after deformation²⁸. Strong texture was observed in the case of MWCNT composites presumably due to the orientation of nanotubes that can help crystalline polymer to align in a preferred orientation. But the plate-shaped RGO was likely unable to easily align in a particular direction during rolling. These effect of the nanoparticles on the crystallographic structure also manifests itself in the nature of the fibrillar morphology of the rolled polymer (Figure 6). The fibrils induced by rolling are most prominently seen along the rolling direction (arrow) in the SEM micrographs of the cryo-fractured surface of PE-R. In CPE-R, the fibrils can also be seen but appear less pronounced than in PE-R. In contrast, GPE-R surface did not exhibit a fibrillar morphology and appears similar to the surfaces of the unrolled samples.

Figure 7 schematically compiles the changes in crystallographic texture induced by rolling. Transformation from orthorhombic to monoclinic transformation essentially

occurs by monoclinic distortion. In monoclinic distortion one axis is compressed and another two axis are expanded and the angle (β) is around 107° . This transformed monoclinic phase also helps in texture strengthening of orthorhombic phase because the second phase also decides the preferred orientation of parent orthorhombic phase. The presence and morphology of the carbonaceous nanoparticles can hinder the evolution of texture. This is observed in GPE-R wherein the RGO particles weaken the texture more so than the MWCNT in CPE-R.

3.3. Mechanical properties

To study the effect of the crystallographic changes on the mechanical properties, the elastic modulus was assessed. The change in modulus was studied as a function of the modifications individually and in combination. Figure 8 presents elastic modulus of the polymer and its two composites before and after rolling. The effect of nanoparticle addition to the PE in the absence of rolling and the effect of rolling of neat PE are plotted along with the moduli for the rolled composites. The elastic modulus increased from 848 MPa in PE to 944 MPa in CPE on addition of MWCNT. In contrast, the modulus of GPE was 1258 MPa. Thus, prior to rolling the addition of RGO was more effective in improving the modulus than an equivalent amount of MWCNT. The increase in modulus was expected because both these carbonaceous nanoparticles are intrinsically strong. When added to the polymer, the stress is transferred to the hard nanoparticles thereby increasing the stiffness. RGO was more effective than MWCNT likely because of the plate-like structure of RGO in contrast to the tube like structure of the latter. Thus, a larger surface area of the filler is available to interact with the polymer matrix to effectively facilitate stress transfer in RGO composites.

Rolling significantly increased the modulus from 850 MPa in PE to 1210 MPa in PE-R. The modulus of CPE increased from 944 MPa to 1110 MPa after rolling. Interestingly, in GPE the modulus decreased from 1258 MPa to 816 MPa after rolling. These observations can be attributed to the effect of addition of these nanoparticles on the evolution of texture during rolling. In CPE, texture strengthening during rolling was higher in both the orthorhombic and monoclinic phases that resulted in significantly increased modulus. Addition of RGO in PE weakened texture intensity thereby reducing the mechanical properties. Thus, the ability of the nanofillers to align in the deformation direction can affect texture evolution thereby determining the mechanical properties.

In light of this, it can be concluded that although controlled crystalline orientation can be induced by hot rolling, the effects in presence of nanoparticles can be very different. More importantly, these effects are also strongly contingent on the shape of the nanoparticles. It is envisaged that rolling induces deformation induced phase transformation in both the composites but the texture intensity decreased significantly in presence of RGO in striking contrast to control PE and MWCNT composites. It is now understood that in semi-crystalline PE, the small amorphous content may not generate sufficient force to cause twinning but compressive forces at elevated temperature can facilitate certain amount of twinning. This presumably explains the texture transition after deformation. Hence, prior to rolling the presence of MWCNTs and RGO has resulted in a wide distribution of spherulites and defective crystals on account of enhanced rate of crystallization. This did not yield a mixture of crystals in PE however, it certainly has increased the amorphous content in PE. The latter was observed to be more prominent in PE with RGO. This hypothesis suggests that in the composite samples involving RGO,

upon rolling, fragmentation of lamellae would occur severely. During viscoelastoplastic deformation, the interfibrillar zones containing amorphous chains and defects when subjected to rolling results in further lamellae fragmentation. In addition to decreased elastic modulus in the RGO-based composite, this is also evident from the less textured microstructure. In the case of MWCNT, the lamellae fragmentation appears to be not as severe as RGO based composites. Moreover, MWCNT presumably orients along the deformation direction. This though did not alter the type of texture in the composites but only moderately increased the elastic modulus. More understanding is needed as to how the presence of nanoparticles impedes the controlled crystalline orientation and more specifically, how the shape of the particles facilitates deformation-induced phase transformation and texture evolution in semicrystalline polymers like PE. These issues are subjected to future investigations.

4. Conclusion

Evolution of crystallographic texture of PE composites containing MWCNT and RGO were characterized when subjected to hot rolling. Deformation induced phase transformation was observed wherein orthorhombic phase transformed into monoclinic phase upon rolling. During rolling RGO but not MWCNT significantly decreased texture intensity of PE. After rolling, elastic modulus increased in case of pure PE and CPE-R but decreased in GPE-R. Ability of CNTs but not RGO to align in the direction of deformation can improve mechanical properties through texture strengthening. The observed crystallographic texture was assessed in light of the fragmented lamellae developed on account of enhanced rate of crystallization in presence of nanoparticles.

Acknowledgement

This work was funded by the Nanomission Program of the Department of Science and Technology (DST), India. K.E. gratefully acknowledges the Department of Biotechnology, India for the Postdoctoral Research Associate fellowship. K.C. acknowledges the Ramanujan fellowship from DST.

References

- 1 M. Matsuo, *ISIJ International*, 1989, 29, 809-827.
- 2 F. Haggag and K. Murty, in *Nondestructive Evaluation and Materials Properties III*, ed. K. Liaw, O. Buck, R. J. Arsenault and R. E. Green Jr., The Minerals, Metals & Materials Society, 1996, pp. 101-106.
- 3 R. Adamesku, *Fizika Metallov i Metallovedenie*, 1987, 63, 987-991.
- 4 S. Li, *Operative Techniques in Orthopaedics*, 2001, 11, 288-295.
- 5 Y. Liu and S. K. Sinha, *Wear*, 2013, 300, 44-54.
- 6 S. Kim, S. Koebel and R. Duffy, *Value in Health*, 2003, 6, 222-223.
- 7 S. R. Kearns, B. Jamal, C. H. Rorabeck and R. B. Bourne, *Clinical Orthopaedics and Related Research*, 2006, 453, 103-109.
- 8 E. Oral, A. L. Neils, C. Lyons, M. Fung, B. Doshi and O. K. Muratoglu, *Journal of Orthopaedic Research*, 2012, 31, 59-66.
- 9 Y. Xue, W. Wu, O. Jacobs and B. Schadel, *Polymer Testing*, 2006, 25, 221-229.
- 10 M. J. Martinez-Morlanes, P. Castell, V. Martinez-Nogues, M. T. Martinez, P. J. Alonso and J. A. Puertolas, *Composites Science and Technology*, 2011, 71, 282-288.
- 11 A. Kaito, K. Nakayama and H. Kanetsuna, *Polym J*, 1982, 14, 757-766.
- 12 E. Gomez-Barrena, J. A. Puertolas, L. Munuera and Y. T. Konttinen, *Acta Orthopaedica*, 2008, 79, 832-840.
- 13 S. H. Naidu, B. L. Bixler and M. J. R. Moulton, *Orthopedics*, 1997, 20, 137-142.
- 14 G. Z. Papageorgiou, Z. Terzopoulou, D. S. Achilias, D. N. Bikiaris, M. Kapnisti and D. Gournis, *Polymer*, 2013, 54, 4604-4616.

- 15 S. Kumar, S. Bose and K. Chatterjee, *RSC Advances*, 2014, 4, 19086-19098.
- 16 S. Bahadur and A. Henkin, *Polymer Engineering & Science*, 1973, 13, 422-428.
- 17 I. L. Hay and A. Keller, *Journal of Materials Science*, 1966, 1, 41-51.
- 18 I. L. Hay and A. Keller, *Journal of Materials Science*, 1967, 2, 538-558.
- 19 D. Lewis, E. J. Wheeler, W. F. Maddams and J. E. Preedy, *Journal of Polymer Science Part A-2: Polymer Physics*, 1972, 10, 369-373.
- 20 M. W. Darlington, B. H. McConkey and D. W. Saunders, *Journal of Materials Science*, 1971, 6, 1447-1464.
- 21 O. Yoda and I. Kuriyama, *Journal of Polymer Science: Polymer Physics Edition*, 1977, 15, 773-786.
- 22 A. Kaito, K. Nakayama and H. Kanetsuna, *Journal of Applied Polymer Science*, 1983, 28, 1207-1220.
- 23 H. Marrs, D. C. Barton, C. Doyle, R. A. Jones, E. L. V. Lewis, I. M. Ward and J. Fisher, *Journal of Materials Science: Materials in Medicine*, 2001, 12, 621-628.
- 24 F. d. r. Addiego, O. Buchheit, D. Ruch, S. Ahzi and A. Dahoun, *Clinical Orthopaedics and Related Research*®, 2011, 469, 2318-2326.
- 25 P. Xavier, K. Sharma, K. Elayaraja, K. S. Vasu, A. K. Sood and S. Bose, *RSC Advances*, 2014, 4, 12376-12387.
- 26 H. Kiho, A. Peterlin and P. H. Geil, *Journal of Applied Physics*, 1964, 35, 1599-1605.
- 27 M. Bevis and E. B. Crellin, *Polymer*, 1971, 12, 666-684.
- 28 S. Tsuneo, H. Tetsuhiko and T. Kenzo, *Japanese Journal of Applied Physics*, 1968, 7, 31-42.

- 29 Y. Chen, Y. Li, H. Zou and M. Liang, *Journal of Applied Polymer Science*, 2013, 131, n/a-n/a.
- 30 A. R. Bhattacharyya, T. V. Sreekumar, T. Liu, S. Kumar, L. M. Ericson, R. H. Hauge and R. E. Smalley, *Polymer*, 2003, 44, 2373-2377.
- 31 I. Y. Phang, J. H. Ma, L. Shen, T. X. Liu and W. D. Zhang, *Polymer International*, 2006, 55, 71-79.
- 32 S. Nikolov, R. A. Lebensohn and D. Raabe, *Journal of the Mechanics and Physics of Solids*, 2006, 54, 1350-1375.

Figure captions:

Figure 1: XRD patterns of PE and the composites before (a) and after rolling (b). Plots of peak intensities before (c) and after rolling (d).

Figure 2: Schematic depiction of orientation relationship in Orthorhombic (parent) and Monoclinic (product) phase.

Figure 3: Pole figures of orthorhombic phase of PE, CPE and GPE.

Figure 4: Pole figures of orthorhombic and monoclinic phases of PE-R, CPE-R and GPE-R.

Figure 5: Plots of pole intensities of orthorhombic and monoclinic phase of PE and the composites (a) before rolling and (b) after rolling.

Figure 6: Representative SEM micrographs of cryo-fractured surface of (a) PE, (b) CPE, (c) GPE, (d) PE-R, (e) CPE-R and (f) GPE-R. The arrow denotes the rolling direction.

Figure 7: Schematic representation of deformation-induced phase transformation in PE during rolling. Black circles represent CH₂ group on (001) plane and the white circles CH₂ group half the periodic distance above or below (001) plane.

Figure 8: Storage modulus of PE and its composites before rolling and after rolling.

Table 1: Lattice parameters of PE phases

Phase	a (Å)	b (Å)	c (Å)	β (°)
Orthorhombic	7.40	4.94	2.53	90.0
Monoclinic	8.09	2.53	4.79	107.9

Table 2: Calculated crystallite size before and after rolling

Sample	FWHM			Crystallite size (Å)		
	(110)	(200)	Monoclinic (001)	(110)	(200)	Monoclinic (001)
PE	0.297	0.341	-	303	264	-
CPE	0.307	0.369	-	293	245	-
GPE	0.329	0.396	-	273	228	-
PE-R	0.446	0.416	0.425	202	217	211
CPE-R	0.483	0.430	0.474	189	210	189
GPE-R	0.485	0.479	0.494	185	189	181

Figure 1

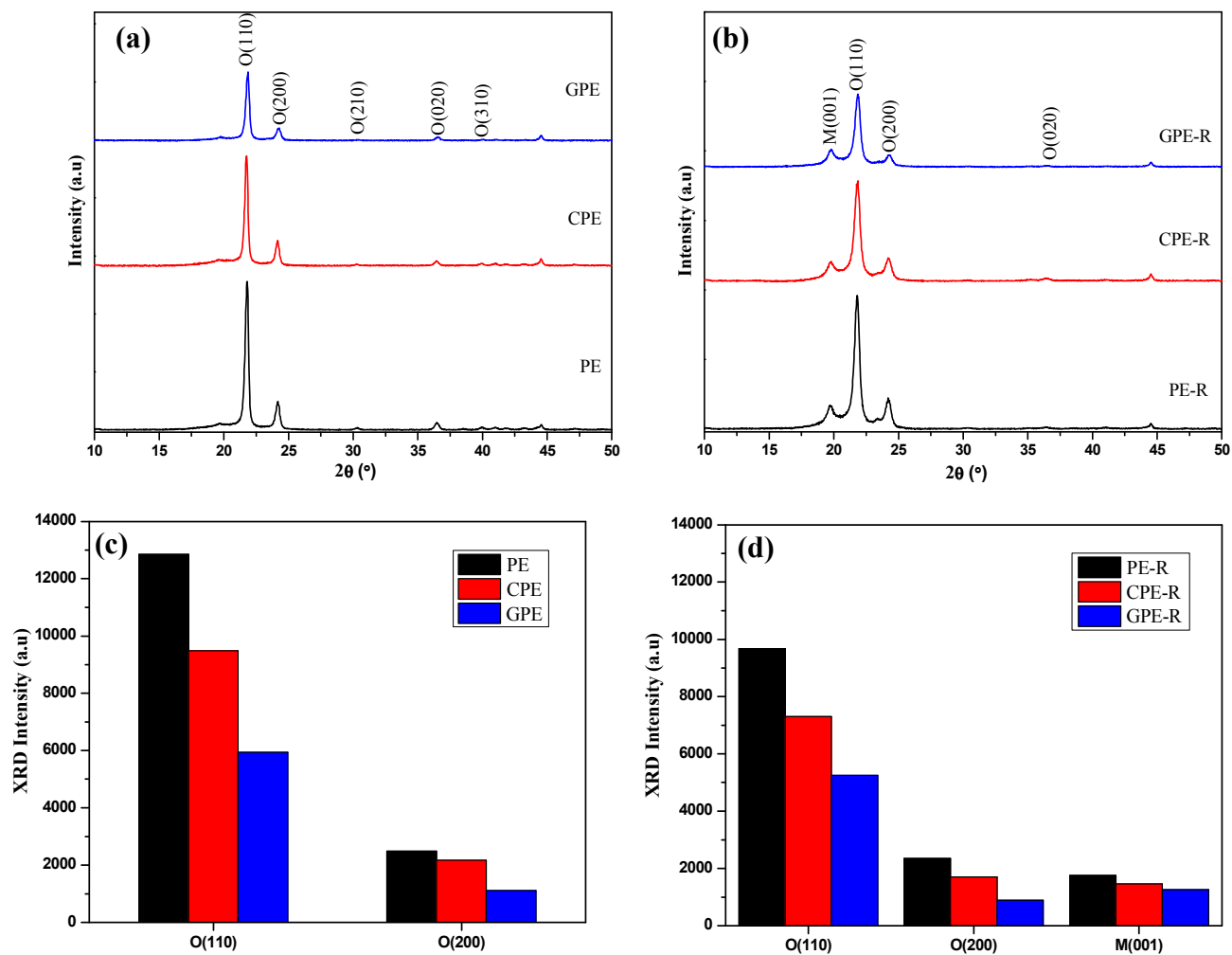


Figure 2

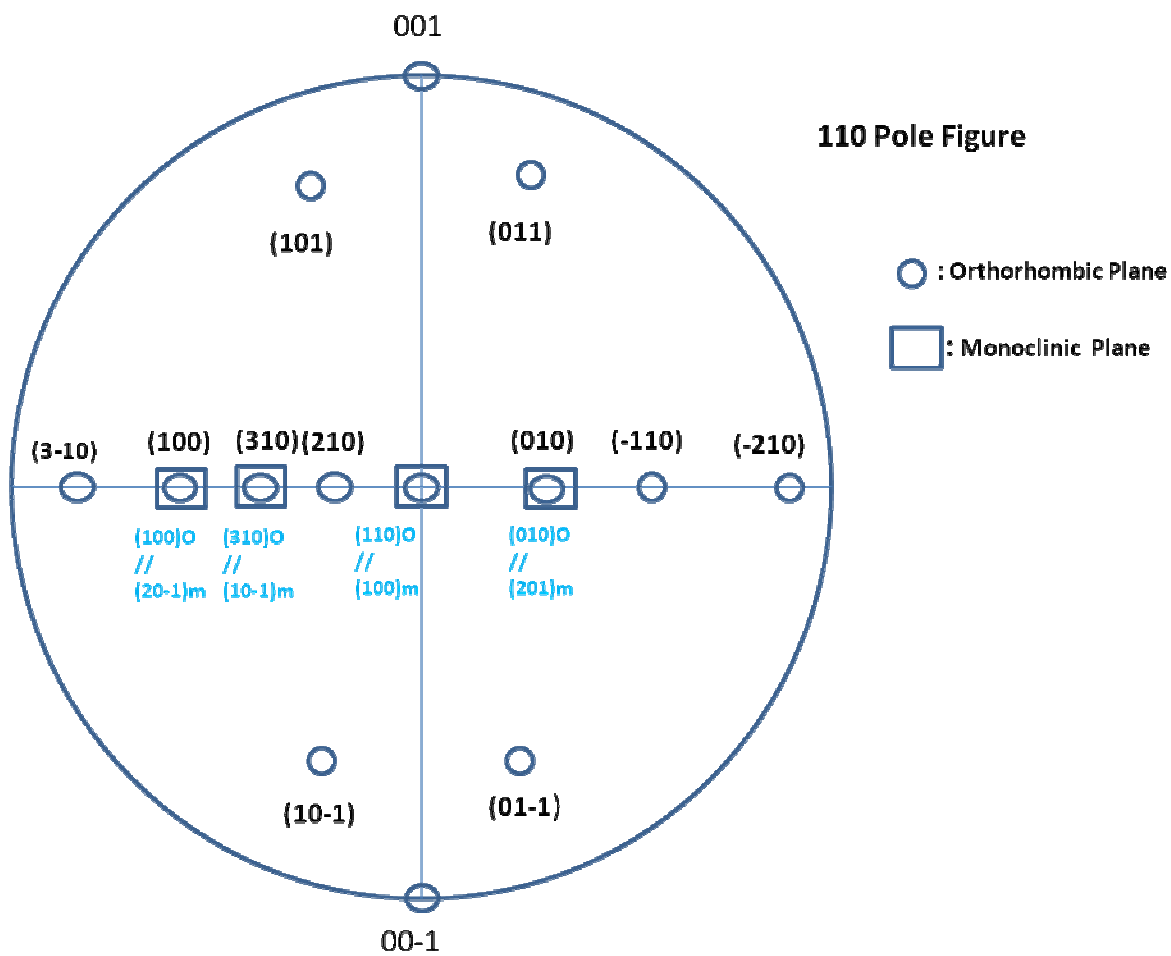


Figure 3

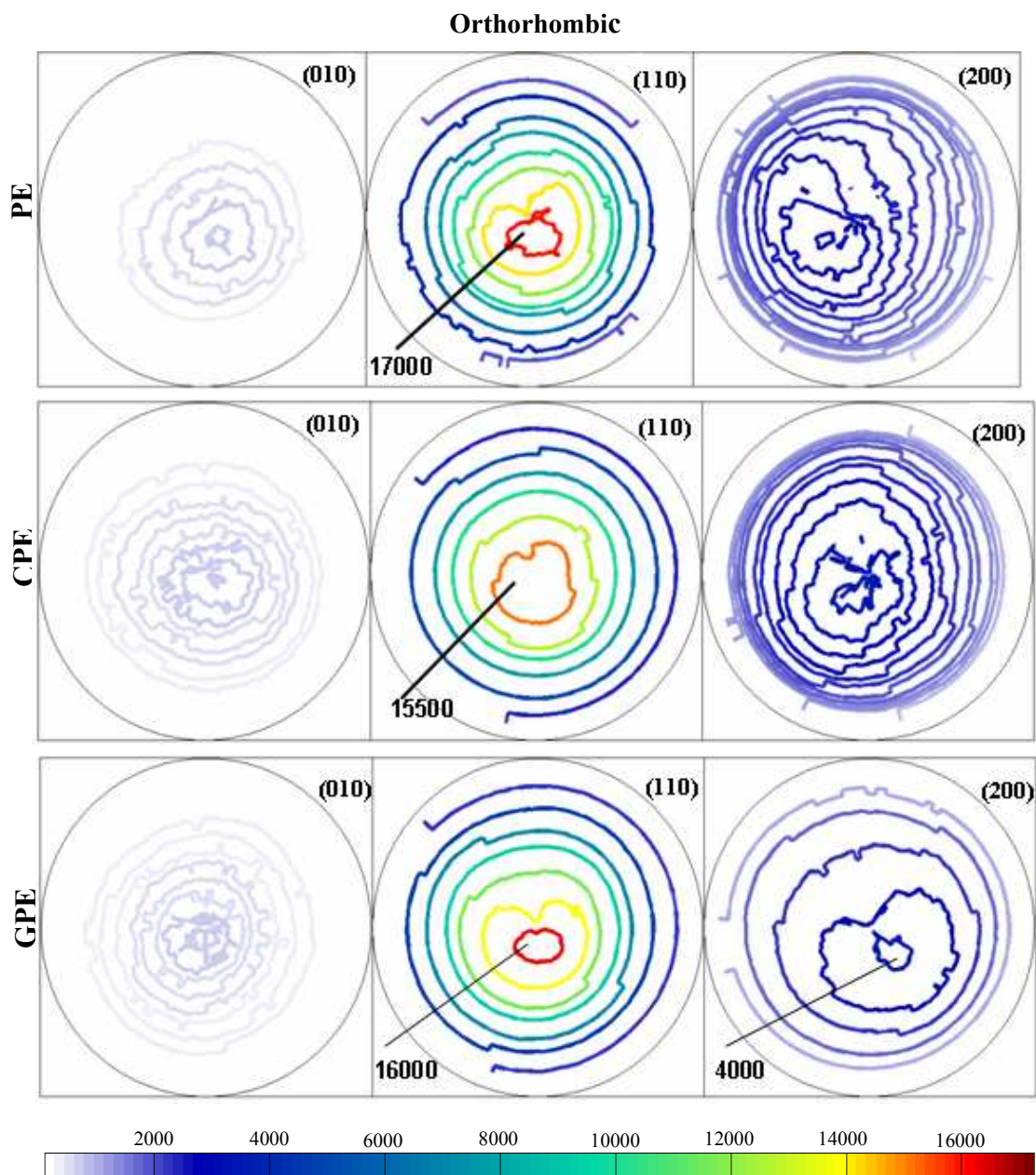


Figure 4

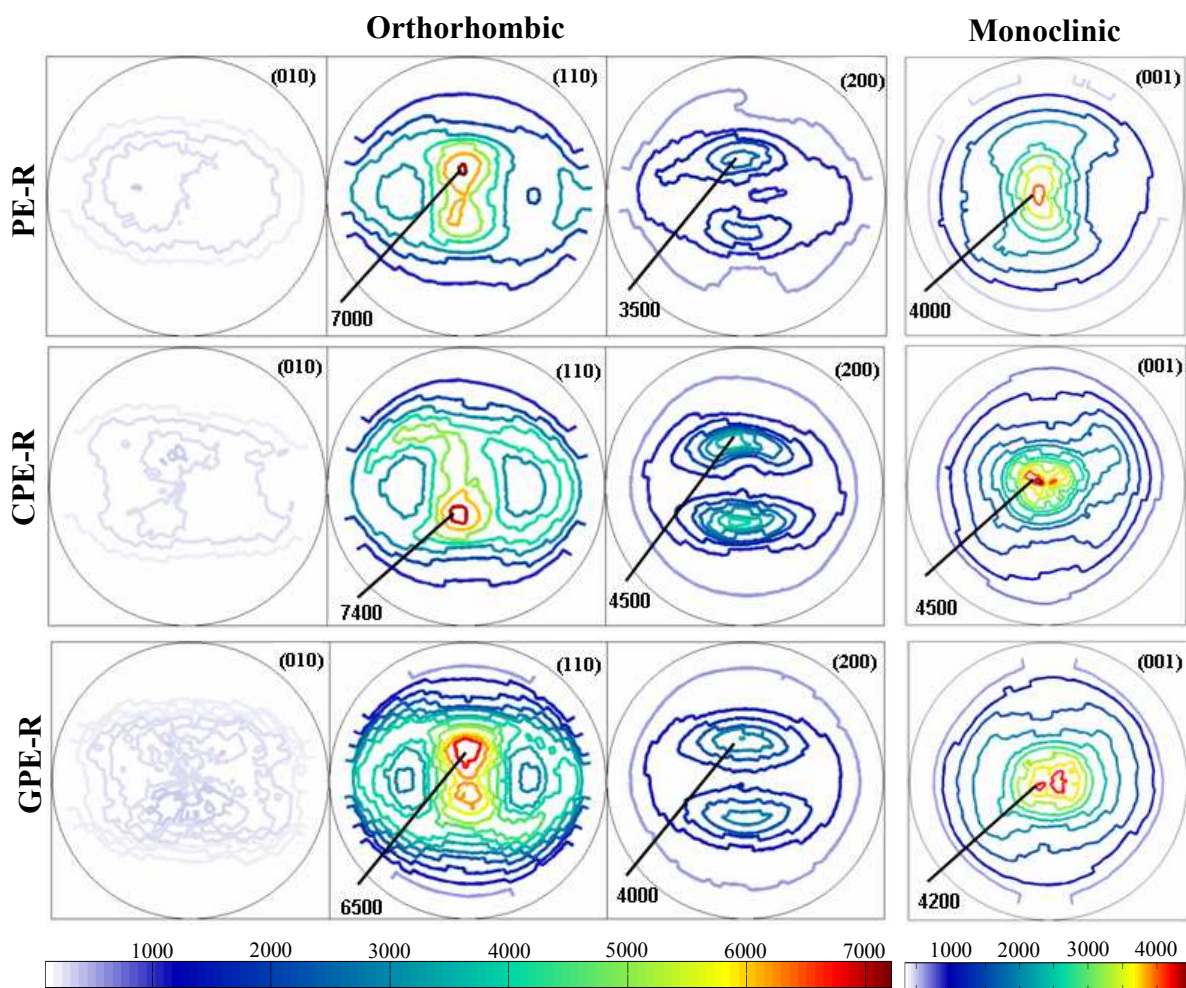


Figure 5

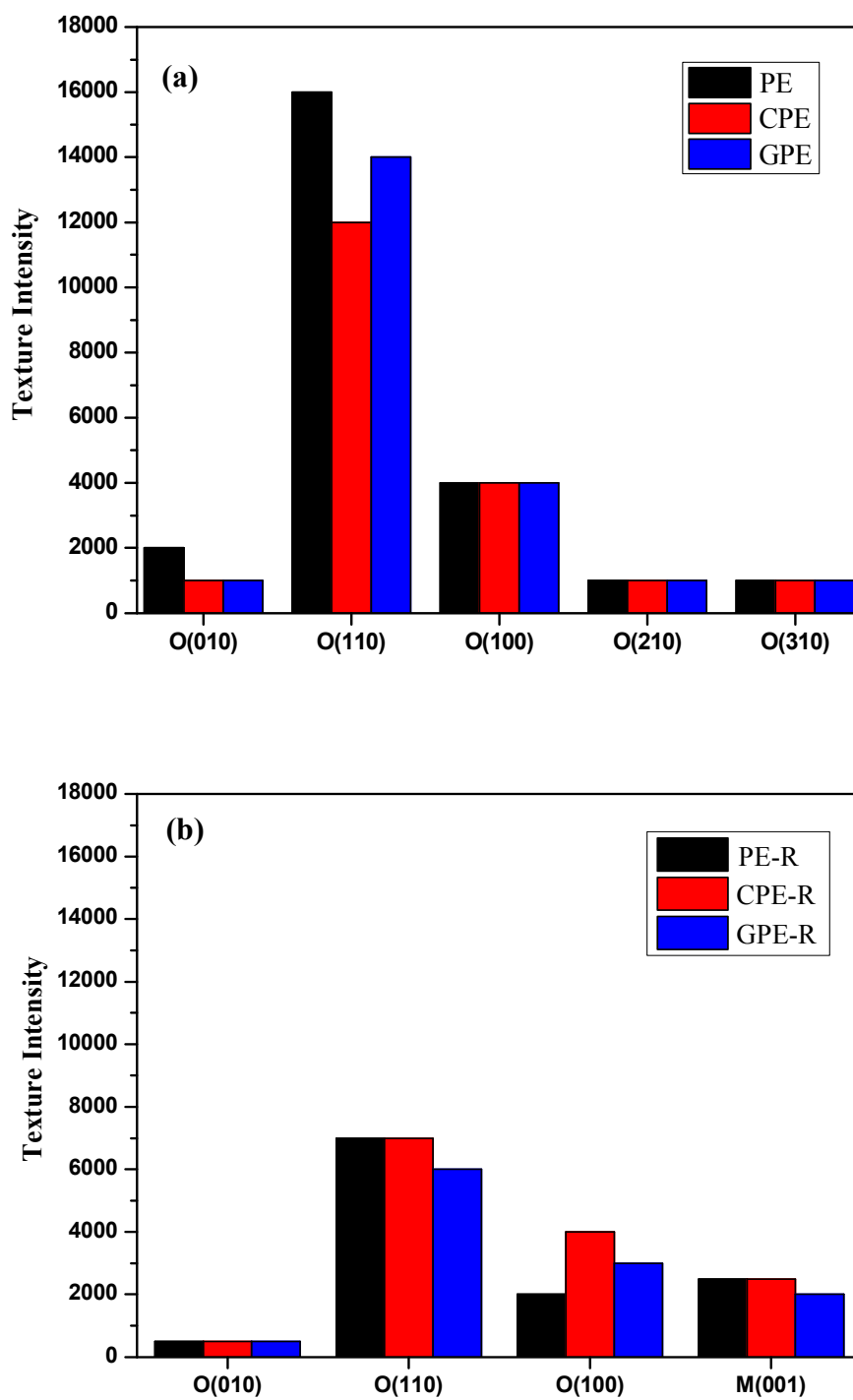


Figure 6

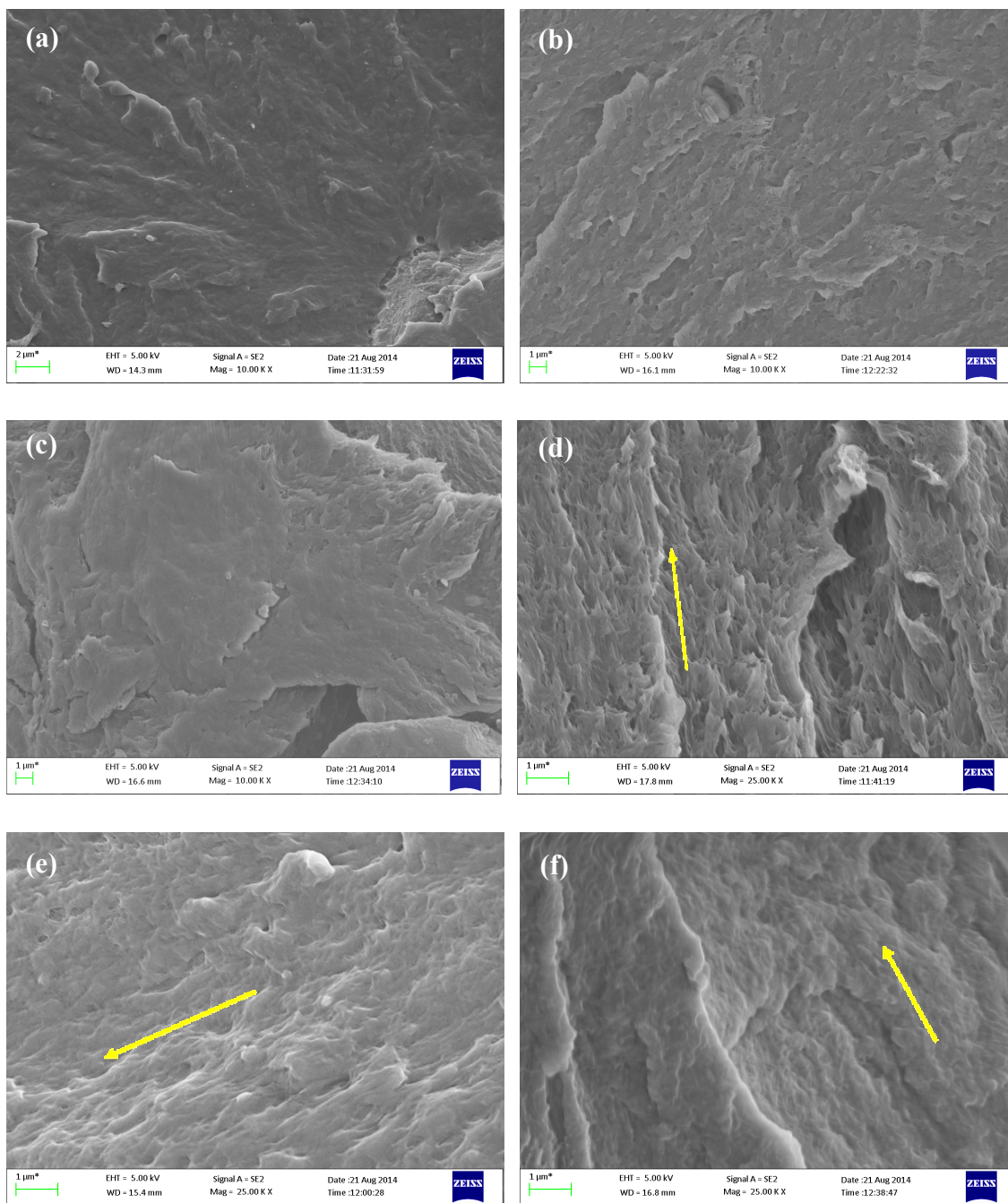


Figure 7

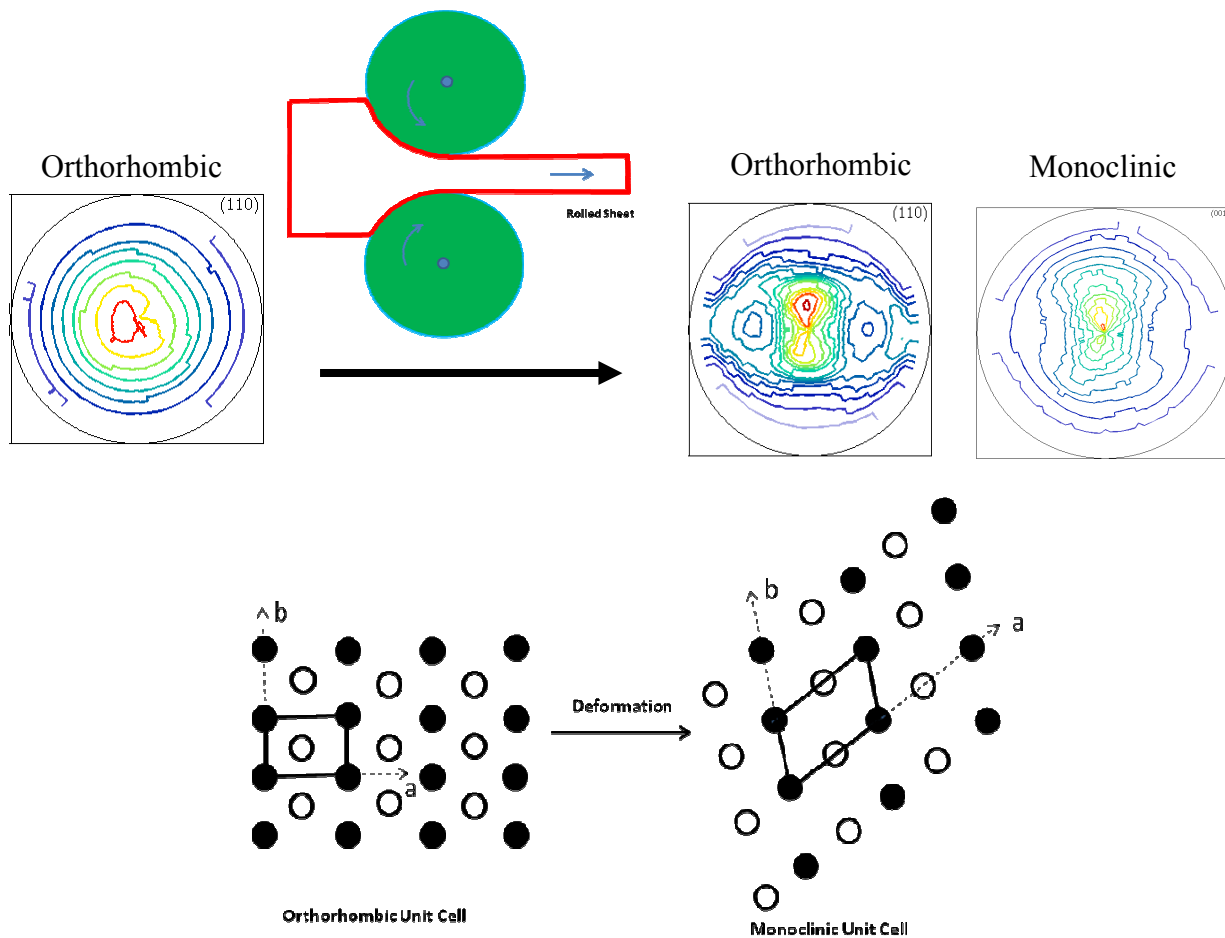


Figure 8

